



Photocatalytic degradation of methyl orange mediated by a silica coated nanomagnet porphyrin hybrid

Kelly A.D.F. Castro^{a,#,*}, João M.M. Rodrigues^{b,#,*}, M. Amparo F. Faustino^a, João P.C. Tomé^c, José A.S. Cavaleiro^a, Maria da Graça P.M.S. Neves^{a,*}, Mário M.Q. Simões^{a,*}

^a LAQV-REQUIMTE, Department of Chemistry, University of Aveiro, 3810-193 Aveiro, Portugal

^b CICECO - Aveiro Institute of Materials, Department of Chemistry, University of Aveiro, 3810-193 Aveiro, Portugal

^c Centro de Química Estrutural, Instituto Superior Técnico, Universidade de Lisboa, Av. Rovisco Pais, 1049-001 Lisboa, Portugal

ARTICLE INFO

Article history:

Received 31 January 2021

Accepted 15 February 2021

Available online 17 February 2021

Keywords:

Porphyrin

Silica nanomagnetic particles

Photocatalysis

methyl orange

Degradation

ABSTRACT

The photocatalytic activity of a silica coated nanomagnet porphyrin hybrid (**NPH**) and of the corresponding porphyrin precursors (**H₂P** and **ZnP**) was evaluated in the degradation of the methyl orange dye (**MO**) under visible light irradiation. The catalytic degradation of **MO** was performed under air, in the absence and in the presence of aqueous hydrogen peroxide. The results show that the hybrid **NPH** was the most effective photocatalyst causing the total degradation of **MO** after 270 min of white light irradiation (150 mW cm⁻²) in the presence of hydrogen peroxide. The remarkable photocatalytic activity of this **NPH**, associated with the possibility of its reuse, makes this material a promising photocatalyst.

© 2021 Elsevier B.V. All rights reserved.

1. Introduction

Environmental pollution is one of the major and most urgent problems of the modern world requiring a constant and special attention from the scientific community. In particular, wastewater from dyeing industries has become exceptionally worrisome, since the presence of dyes can inhibit sunlight penetration and, consequently, might reduce the photosynthetic process [1,2]. Following these inputs, the scientific community is contributing with the development of novel and economically sustainable methodologies for the detoxification of textile wastewaters, aiming to follow the recommended quality criteria and to close the water cycle [3,4].

The large-scale use of dyes results in the production of large volumes of pollutants, which are often discarded without any previous treatment. Therefore, the development of efficient methodologies in order to minimize the environmental impact caused by industrial effluents is of great interest [5]. Different methodologies have been developed for the degradation and/or scavenging of those dyes, especially azo dyes (the most common synthetic dyes, ca 70% wt.). These methodologies include adsorption, biological oxidation, membrane filtration, ozonation, oxidation using UV/H₂O₂, UV/TiO₂, UV or visible light and catalysis [3,6–9]. The

approaches based on catalytic processes appear as important alternatives in the remediation of effluents. In fact, the fundamental pillar of green chemistry is catalysis, generally resulting in significant gains in terms of overall efficiency of a chemical reaction. Porphyrins and analogues are among the catalysts with recognized efficacy for azo dyes (photo)degradation [1,5,10].

Metalloporphyrins and analogues have already proved their efficiency as catalysts, namely for oxidative reactions [11–20]. Porphyrins are also efficient producers of reactive oxygen species (ROS) in the presence of light, such as singlet oxygen (¹O₂) [21–24], thus inducing many photocatalytic reactions [25,26]. The reaction of ROS with the target pollutants is an alternative method for removing organic pollutants [27,28]. From the successful history of photocatalysts, the special attention given to porphyrins and analogues by the scientific community is due to their strong absorption bands in the visible region, versatile chemical structures, and facile tuning of the electronic properties. Besides, the insertion of diverse metals into the core of the macrocycle can modulate the catalytic activity associated with the porphyrins' structure. Additionally, the development of heterogeneous catalysts based on porphyrins represents an important challenge for a sustainable development.

Recently, magnetite nanoparticles (Fe₃O₄) have originated a great interest due to their physicochemical characteristics. Fe₃O₄ with different structures has been used in different areas, such as environmental technology, nanotechnology, medicine and catalysis [29–33]. In addition to their exceptional

* Corresponding authors.

E-mail addresses: kadfc16@gmail.com (K.A.D.F. Castro), jrodrigues@ua.pt (J.M.M. Rodrigues), gneves@ua.pt (M.d.G.P.M.S. Neves), msimoes@ua.pt (M.M.Q. Simões).

These two authors contributed equally to this work.

variety of applications, magnetite nanoparticles have the advantage of their possible reuse. For instance, Qin and co-workers studied $\text{Fe}_3\text{O}_4/\text{TiO}_2$ magnetic nanoparticles for photocatalytic degradation of phenol [34]. In another study, it was reported the synthesis and characterization of magnetic nanoparticles functionalized with [5,15-bis(phenyl)-10,20-bis(4-methoxycarbonylphenyl)porphyrin]platinum(II) and the photocatalytic activity of the hybrid was tested using 2,4,6-trichlorophenol as the target pollutant [35]. More recently, magnetite nanoparticles with different morphologies (cubic and spherical ones) decorated with the 5,10,15,20-tetrakis(4-carboxyphenyl)porphyrin showed to be able to generate $^1\text{O}_2$ under ultraviolet irradiation. Their study as photocatalysts towards bisphenol A (BPA) disclosed degradation values of 64% (cubic-shaped) and of 90% (spherical shape) in the presence of hydrogen peroxide (H_2O_2) [36]. Additionally, these materials retained their catalytic features for at least three catalytic cycles.

Following our interest in developing new materials for environmental remediation, in this publication we report the synthesis and characterization of core-shell magnetite-silica nanoparticles functionalized with the Zn(II) complex of a porphyrin obtained from the reaction of 5,10,15,20-tetrakis(pentafluorophenyl)porphyrin with tosylthylenediamine. Furthermore, the efficacy of this material to act as photocatalyst was evaluated under white light irradiation (380-750 nm) using methyl orange dye (MO) as the target pollutant. The studies were performed under air in the absence and in the presence of aqueous H_2O_2 .

2. Experimental

2.1. Reagents and Equipment

All chemicals used in this study were purchased from Sigma-Aldrich or Merck and were of analytical grade.

Electronic spectra (UV-Vis) were obtained on a Shimadzu UV-2501PC spectrophotometer, in the 350-800 nm range. The fluorescence emission spectra were recorded in DMF in 1×1 cm quartz optical cells at 298 K under normal atmospheric conditions on a computer-controlled Horiba Jobin Yvon FluoroMax-3 spectrofluorimeter. The widths of both excitation and emission slits were set at 2.0 nm. ^1H and ^{19}F NMR spectra were recorded on a Bruker Avance AMX 300 spectrometer at 300.13 MHz and 282.38 MHz, respectively. Deuterated dimethylsulfoxide was used as solvent and TMS ($\delta = 0$ ppm) as the internal standard; chemical shifts are reported in ppm (δ) and coupling constants (J) are given in Hz. Mass spectra were acquired on an Applied Biosystems Analyzer mass spectrometer (MALDI TOF/TOF). HRMS-ESI spectra were recorded on VG AutoSpec-M spectrometer.

2.2. Preparation of porphyrins H_2P and ZnP

The porphyrins were prepared according to the following steps:

- The precursor 5,10,15,20-tetrakis(pentafluorophenyl)porphyrin [$\text{H}_2(\text{TPFPP})$] was synthesized by condensation of pyrrole with pentafluorobenzaldehyde under acidic conditions [11,37].
- The tri-substituted free-base porphyrin (H_2P) was obtained by structural modification of [$\text{H}_2(\text{TPFPP})$] in the presence of the nucleophile *N*-tosylethylenediamine, as described in the literature [38].
- The Zn(II) complex of H_2P (ZnP) was obtained by adding zinc(II) acetate (42.1 mg, 0.32 mmol) to a solution of H_2P (50.0 mg) in dichloromethane/methanol (2:1, 15 mL) and the resulting mixture was refluxed at 60 °C for 1 h (Scheme 1). After cooling to room temperature, the reaction mixture was washed

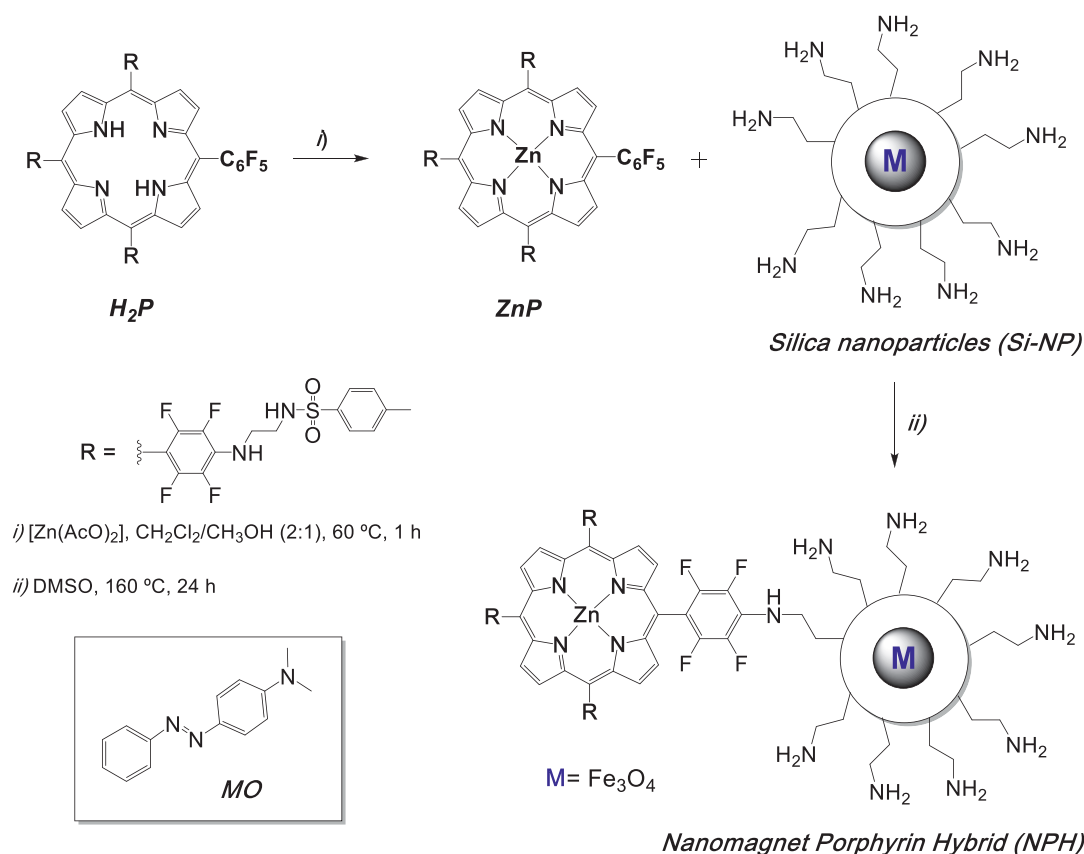
with distilled water. The organic phase was dried (Na_2SO_4) and the solvent was evaporated under reduced pressure. The ZnP was obtained in quantitative yield by crystallization in dichloromethane/hexane.

H_2P : Yield: 19%; ^1H NMR (DMSO- d_6): δ -3.13 (s, 2H, NH), 2.37 (s, 9H, Ts- CH_3), 3.18 (q, $J = 6.2$ Hz, 6H, CH_2), 3.64 (q, $J = 6.2$ Hz, 6H, CH_2), 6.47 (s, 3H, NH- PhF_4), 7.47 (d, $J = 8.2$ Hz, 6H, Ts-*o*-H), 7.81 (d, $J = 8.2$ Hz, 6H, Ts-*m*-H), 7.90 (t, $J = 6.1$ Hz, 3H, NH-Ts), 9.24-9.33 (m, 8H, H- β) ppm. ^{19}F NMR (DMSO- d_6): δ -163.08 to -162.97 (m, 2F, *o*-F), -166.67 (d, $J = 18.4$ Hz, 6F, Ts-*o*-F), -177.52 (t, $J = 22.4$ Hz, 1F, *p*-F), -183.67 to -183.77 (m, 6F, Ts-*m*-F), -186.43 to -186.25 (m, 2F, *m*-F). **UV-Vis** (CHCl_3), λ_{max} (log ϵ): 421 (5.36), 511 (4.26), 548 (3.64), 586 (3.86), 653 (3.42). **UV-Vis** (DMSO), λ_{max} : 424, 512, 548, 586, 648 nm. **HRMS-ESI:** Calculated for $\text{C}_{71}\text{H}_{50}\text{F}_{17}\text{N}_{10}\text{O}_6\text{S}_3$ [$\text{M}+\text{H}$] $^+$ 1557.2805; found: 1557.2587.

ZnP : ^1H NMR (DMSO- d_6): δ 2.36 (s, 9H, Ts- CH_3), 3.16 (q, $J = 6.0$ Hz, 6H, CH_2), 3.61 (q, $J = 6.0$ Hz, 6H, CH_2), 6.39 (s, 3H, NH- PhF_4), 7.47 (d, $J = 8.2$ Hz, 6H, Ts-*o*-H), 7.81 (d, $J = 8.2$ Hz, 6H, Ts-*m*-H), 7.91 (t, $J = 6.0$ Hz, 3H, NH-Ts), 9.07-9.16 (m, 8H, β -H). ^{19}F NMR (DMSO- d_6): δ -162.78 to -162.87 (m, 2F, *o*-F), -166.22 (d, $J = 17.8$ Hz, 6F, Ts-*o*-F), -178.23 (t, $J = 22.4$ Hz, 1F, *p*-F), -184.06 (dd, $J = 17.8$ and 10.1 Hz, 6F, Ts-*m*-F), -186.73 to -186.92 (m, 2F, *m*-F). **UV-Vis** (CHCl_3), λ_{max} (log ϵ): 418 (5.24), 513 (4.24), 580 (3.43) nm. **UV-Vis** (DMSO), λ_{max} : 420, 520, 586 nm. **MS (MALDI TOF/TOF)** (m/z): 1620.0 [$\text{M}+\text{H}$] $^+$.

2.3. Preparation of the Nanomagnet Porphyrin Hybrid (NPH) material

The Nanomagnet Porphyrin Hybrid (NPH) material was prepared according to the procedure described in the literature [39]. Briefly, the magnetic cores (magnetite) were synthesized by the coprecipitation method under basic conditions using ammonium hydroxide. Then, the cores after being coated with silica using the silicic acid approach were maintained under stirring for 24 h in the presence of (3-aminopropyl)triethoxysilane (APTS) in order to obtain the desired nanoparticles functionalized with aminopropyl chains. The magnetic aminopropyl silica nanoparticles (**Si-NP**) were filtered, washed several times with ethanol, followed by magnetic decantation purification. Subsequently, the immobilization of the porphyrin ZnP into **Si-NP** was performed. For this, a previously prepared ethanol suspension of the **Si-NP** [39] (13.5 mL, corresponding to 250 mg of **Si-NP**) were filtered through a polyamide membrane, washed several times with DMSO and re-suspended in DMSO (6 mL). A solution of ZnP (20.0 mg, 12.3 μmol) in DMSO (2 mL) was added to the previous **Si-NP** suspension and the resulting mixture was stirred for 24 h at 160 °C (Scheme 1). The immobilization of ZnP was easily monitored by thin-layer chromatography since the disappearance of the spot corresponding to ZnP was accompanied by the concomitant appearance of a spot corresponding to the **NPH** material at the application point. The insoluble material with a violet color was washed several times with appropriate solvents: firstly, dichloromethane and then a mixture of dichloromethane/methanol (90:10) until the Soret band of the ZnP was no longer detected through UV-Vis in the rinsing solvent. The quantification of the non-immobilized ZnP present in the washing solvents allowed to calculate the ZnP loading in the material (based on the ϵ value of the Soret band of ZnP). In the washing process, the hybrid material **NPH** in DMSO was firstly decanted by recurring to a magnet and then filtered under vacuum, using a polyamide membrane on a Büchner funnel. The **NPH** material was re-suspended and kept in dry DMSO (25 mL), making a stock solution of the **NPH** photocatalyst for the photocatalytic activity assays. **NPH** was characterized by UV-Vis and fluorescence spectroscopy.



Scheme 1. Synthetic procedure used to obtain the Nanomagnet Porphyrin Hybrid (**NPH**) and the structure of methyl orange (**MO**) used as azo dye model.

2.4. Singlet oxygen generation

Stock solutions of each porphyrin (**H₂P** and **ZnP**) and of 1,3-diphenylisobenzofuran (DPIBF) in DMF at 0.1 mM and 10 mM, respectively, were prepared. The reaction mixture containing DPIBF (50 μM) and a solution of each photocatalyst (0.5 μM) in DMF was irradiated in a quartz cell (3 mL), under magnetic stirring at an irradiance of 10 mW cm⁻² with a homemade LEDs array. The LEDs array is composed of a matrix of 5 × 5 LEDs making a total of 25 light sources with an emission peak centered at 654 nm and a bandwidth at half maximum of ± 20 nm. During the irradiation period the solutions were stirred at ambient temperature. The DPIBF degradation was monitored by measuring the absorbance decrease at 415 nm at irradiation intervals of 1 min. The percentage of decay of DPIBF absorption is related with the production of singlet oxygen. The quantification was achieved by the difference between the initial and the final absorbance at 415 nm over a given irradiation time. The same strategy was adopted for **NPH**, but the photocatalyst concentrations used were 0.5, 1.0, 2.0, and 5.0 μM. The results obtained were compared with those obtained in the presence of **H₂TTP** (5,10,15,20-tetraphenylporphyrin) and in the absence of any porphyrin (negative control) under similar irradiation conditions.

2.5. Photocatalytic activity

The photocatalytic activity of **H₂P**, **ZnP** and **NPH** was evaluated in aqueous solutions using methyl orange (**MO**) as model substrate and under visible light irradiation, which was performed with a halogen 500 W lamp at an irradiance of 150 mW cm⁻². This light source was positioned 10 cm away from the batch reactor and the temperature was kept at ca 20 °C under stirring. The reactions were performed under air and in the presence of aqueous H₂O₂.

A stock solution of the dye ([**MO**] = 8.26 × 10⁻² mol L⁻¹) was prepared in milli-Q water. To a 4 mL quartz cuvette, 3.0 mL of water, 200 μL of **MO** dye solution and the adequate volume of stock solution of the catalyst (**H₂P** or **ZnP** in DMSO) were added to obtain a final concentration of 0.5 μM. For the reactions carried out in the presence of hydrogen peroxide, 100 μL of aqueous H₂O₂ (30%, w/w) were added. In the case of the heterogeneous photocatalyst (**NPH**), the solution was stirred in the dark (30 min) before irradiation in order to obtain an equilibrium point of initial physical adsorption of **MO** over the surface of the photocatalyst. All photocatalytic experiments were accomplished under similar conditions. The photocatalytic performance was monitored indirectly by relating the decrease in the absorbance of **MO** at 464 nm in solution with its degradation. The photocatalytic reactions in the presence of hydrogen peroxide were also performed in the presence of mannitol. The production of •OH radicals was investigated indirectly by degradation of terephthalic acid (TA) [40]. The reaction mixture containing TA (1 mM) and a solution of each photocatalyst (0.5 μM **H₂P**, 0.5 μM **ZnP** and 5.0 μM of **ZnP** in **NPH** in PBS solutions (pH = 7.0) with 1% DMSO and 100 μL of aqueous H₂O₂ (30%, w/w) was irradiated in a quartz cell (4 mL) with white light at an irradiance of 150 mW cm⁻². The reaction mixture was stirred in the dark (30 min) before irradiation. The TA degradation was monitored by measuring the emission at 450 nm (λ_{exc} = 315 nm) for 60 min of irradiation. Dark controls were included.

3. Results and Discussion

3.1. Synthesis and characterization of the photocatalysts

The synthetic methodology used in the preparation of the homogeneous and the heterogeneous photocatalysts is summarized in **Scheme 1**. The porphyrin derivative **H₂P** was prepared by a

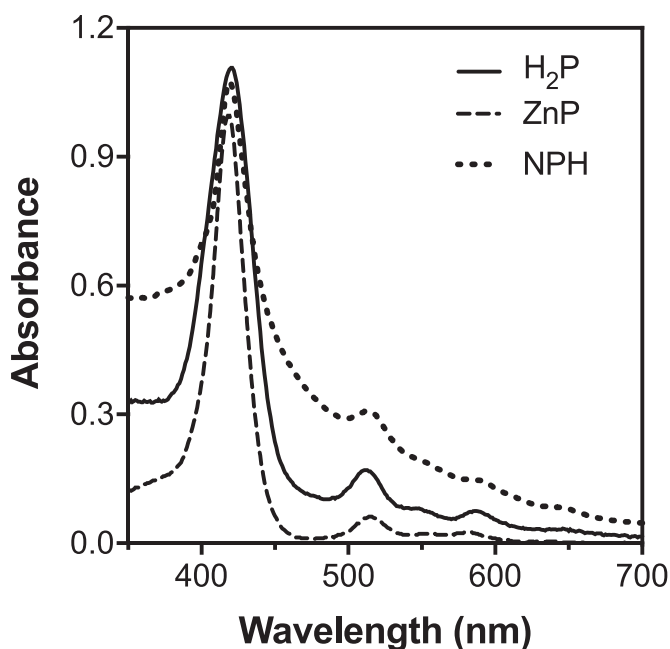


Fig. 1. UV-Vis spectra of **H₂P**, **ZnP** and **NPH** in DMSO.

controlled nucleophilic substitution of three of the *p*-fluorine atoms in **H₂(TPFPF)** with *N*-tosylethylenediamine, according to the procedure reported previously by our group [38]. The subsequent reaction of **H₂P** with zinc(II) acetate in dichloromethane:methanol (2:1) at 60 °C afforded the corresponding **ZnP** complex (Scheme 1). The structural confirmation of both derivatives **H₂P** and **ZnP** was performed by recurring to adequate spectroscopic techniques namely ¹H NMR, mass spectrometry (Figures S1-S5 in the Supporting information) and UV-Vis spectroscopy.

The covalent immobilization of **ZnP** onto the core-shell magnetite silica nanoparticles (**Si-NP**) functionalized with amino groups occurred via nucleophilic substitution of the *p*-fluorine atom at the C₆F₅ group and was performed in DMSO at 160 °C for 24 h; the functionalized nanoparticles **Si-NP** were obtained by reacting the magnetic cores covered with silica with APTS according with literature procedures [39,41]. After the immobilization step, the obtained violet nanoparticles were thoroughly washed with appropriate solvents affording the desired **NPH**, the **ZnP** loading in the **NPH** found was 3.37×10^{-4} mol g⁻¹. This loading was determined by quantifying the amount of the non-immobilized **ZnP** by UV-Vis in the rinsing solutions. Then, the **NPH** was re-suspended in DMSO and the success of the immobilization was confirmed by UV-Vis and fluorescence spectroscopy.

The UV-Vis spectra of **H₂P**, **ZnP** and of the **NPH** suspension in DMSO are displayed in Fig. 1. The non-immobilized porphyrin derivatives **H₂P** and **ZnP** show the typical Soret band at 424 and 420 nm, respectively, accompanied by the less intense Q bands at 512, 548, 586, and 648 nm for **H₂P** and at 520 and 586 nm for **ZnP**; this decrease in the number of the Q bands after metalation is related to the alteration in the micro symmetry of the porphyrin macrocycle. In the magnetic hybrid **NPH** the presence of **ZnP** complex was promptly confirmed by the appearance of the Soret band at 419 nm and of the corresponding Q-bands at 515 and 580 nm. These features validated the success of the immobilization and the UV-Vis spectrum profile is similar to that obtained for the non-immobilized **ZnP** in solution. Additionally, the UV-Vis spectra were also acquired in a mixture of DMSO:H₂O and are shown in the SI (Figure S6). As it is expected the spectrum of the silica nanoparti-

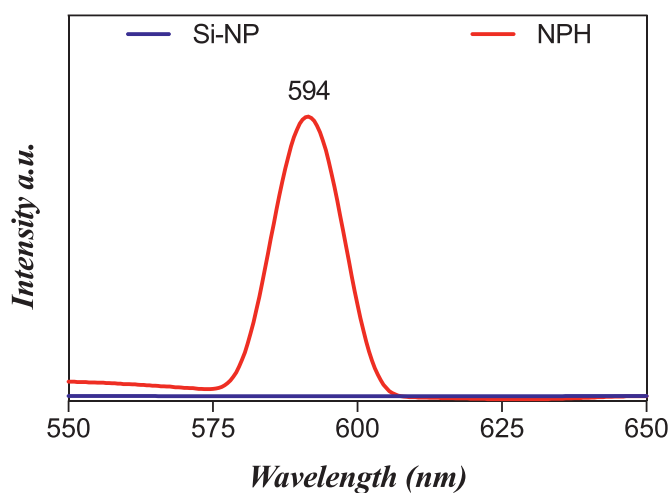


Fig. 2. Emission spectra of **Si-NP** and **NPH** in DMSO solution.

cles (**Si-NP**) did not present bands in the region of 400 nm (Figure S6).

The presence of **ZnP** in the hybrid was also confirmed by the emission spectrum obtained of the **NPH** material in DMSO solution upon excitation at 410 nm (Fig. 2). The strong emission band observed in the red region at ca. 594 nm [$\lambda > Qx(0,0)$] can only be due to immobilized **ZnP** since the **Si-NP** did not present any emission band upon 410 nm excitation. Similar results were observed for other porphyrin derivatives when immobilized [42].

3.2. Singlet oxygen generation

The ability of photocatalysts to generate ROS, namely singlet oxygen (¹O₂), superoxide anion radical (O₂^{•-}), hydrogen peroxide (H₂O₂) and hydroxyl radical ([•]OH) is considered a crucial feature regarding their efficiency in photocatalysis [43]. In general, when porphyrin derivatives are used as photocatalysts, ¹O₂ is the major ROS involved [25]. The production of ¹O₂ was assessed by an indirect chemical method using 1,3-diphenylisobenzofuran (DPIBF) as a probe. As other furans, this compound is able to react as a diene in a [4+2] process with ¹O₂ as the dienophile affording the colorless *o*-dibenzoylbenzene; with this quencher, exclusively ¹O₂ is detected [44].

So, the photodegradation of DPIBF mediated by **H₂P**, **ZnP**, **NPH** and also by **H₂TPP** (used as reference) was qualitatively assessed by monitoring its absorbance decay at 415 nm as a function of the irradiation time with red light (654 ± 20 nm). The results in Fig. 3 show that the absorbance of DPIBF at 415 nm decreased in the presence of all porphyrin derivatives under irradiation as a function of time through a 1st kinetic order. Comparing the photodecomposition slope promoted by each porphyrin is observed that **H₂P** was the best ¹O₂ generator, being even better than the reference (**H₂TPP**), followed by **ZnP** and **NPH**. For **NPH**, a significant increase of ¹O₂ production was observed when its concentration was increased from 0.5 to 5 μM.

This observation was important in order to establish the amount of material required for the photocatalytic reactions. This reduction in ¹O₂ production is in accordance with other studies involving silica nanoparticles or others nanoplatforms where the ¹O₂ production by the porphyrin immobilized is significantly reduced [45].

The photostability and the solubility of the catalyst in solution are important for homogeneous catalysis. The photostability of **H₂P**, **ZnP** and **NPH** were investigated by UV-Vis, monitoring the absorbance of the corresponding Soret band after different times of

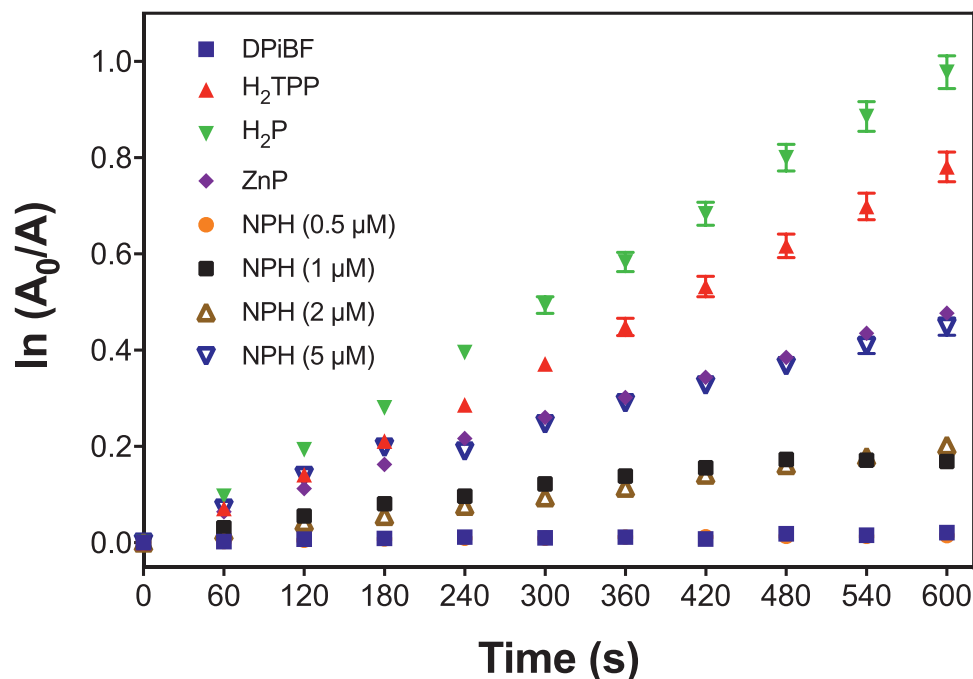


Fig. 3. Time dependent photodecomposition of DPiBF (50 μM) in DMF upon irradiation with red light (654 ± 20 nm) in the absence (DPiBF) or in the presence of H₂P, ZnP and NPH (0.5 μM for H₂P, ZnP and H₂TPP and 0.5, 1.0, 2.0 and 5.0 μM of ZnP on NPH). H₂TPP was used as reference. Note: Small bars are overlapped by the symbols.

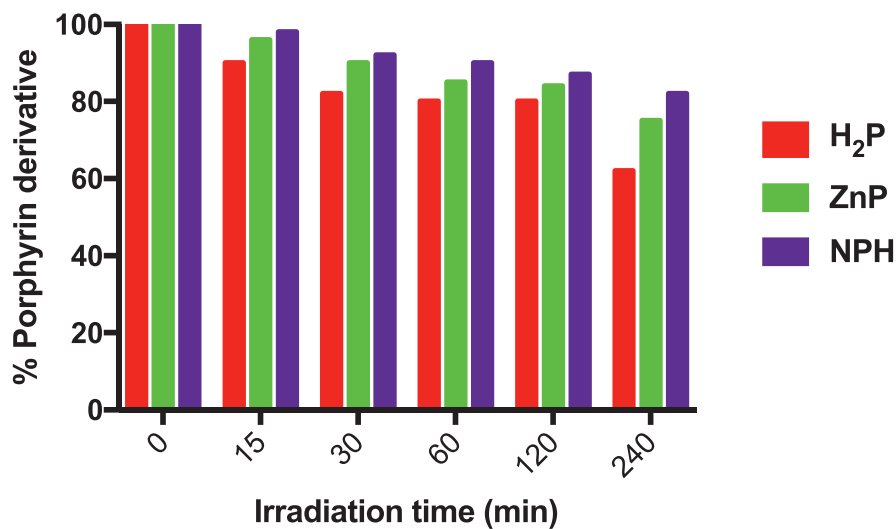


Fig. 4. UV-Vis spectroscopy study of H₂P, ZnP and NPH at a concentration of 5.0 μM in DMSO/water before and after white light irradiation at an irradiance of 150 mW cm⁻² at different irradiation times (0 - 240 min).

irradiation (Fig. 4). In all cases, a good photostability was observed under the photocatalytic studies conditions.

3.3. Photocatalytic activity

The photocatalytic activity of H₂P, ZnP and NPH was evaluated using MO as an azo dye model due to its resistance to environmental degradation. The experiments were performed under white light irradiation (380-750 nm) under air, and in the absence or in the presence of aqueous H₂O₂ as oxidant. The degradation of MO in the presence of H₂P, ZnP and NPH was monitored by measuring the decay of MO absorbance band at 464 nm. The photocatalytic efficiency of the different materials was expressed using the following equation: $(A_0 - A_t)/A_0$, where A_0 is the absorbance of MO

in the reaction mixture at time zero and A_t is the MO absorbance at an established time (t).

The catalysts H₂P, ZnP and NPH showed significant differences ($p < 0.05$) in terms of dye degradation efficiency when the irradiations were performed without H₂O₂ (Fig. 4). NPH was the most efficient photocatalyst causing a reduction of 54% in MO dye concentration after 240 min of irradiation when compared with H₂P and ZnP which attained a maximum of ca 12% under the same irradiation period. In addition, the catalytic reactions were carried out in the absence of white light irradiation (dark conditions), and the MO degradation was not observed in the presence of none of the photocatalysts (H₂P, ZnP and NPH) under dark conditions, as well as for both controls (dark and light).

The results obtained when the experiments were repeated in the presence of H₂O₂ are summarized in Figs. 6 and 7, in the dark

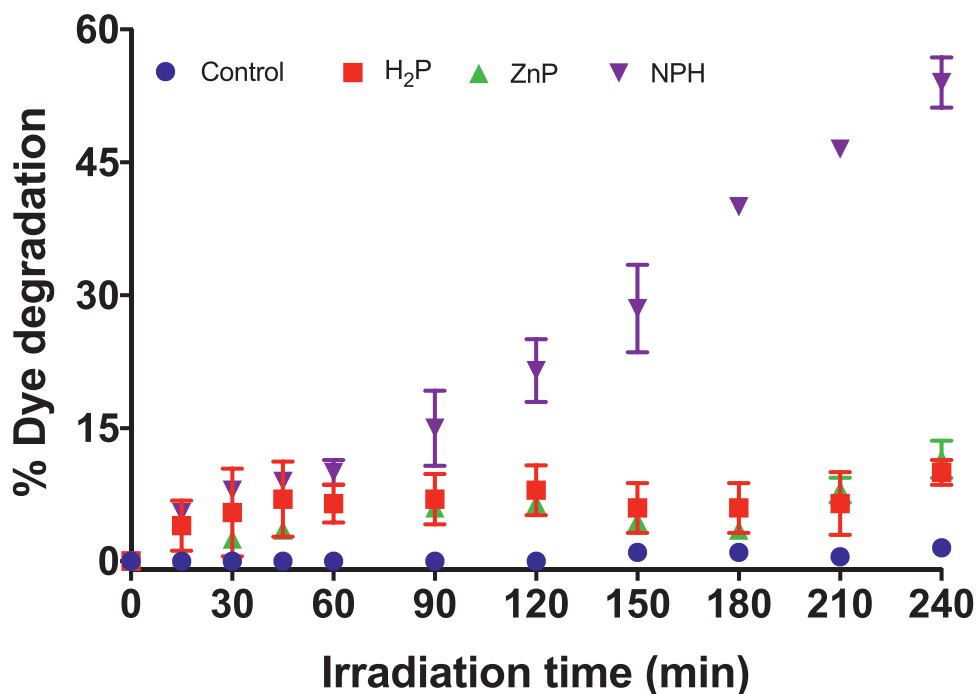


Fig. 5. Photocatalytic degradation of methyl orange (MO) under air at different photoreaction times under light irradiation (150 mW cm^{-2}): in the presence of $0.5 \text{ }\mu\text{M}$ of H_2P (red shape) and ZnP (green shape); $5.0 \text{ }\mu\text{M}$ of ZnP in NPH (purple shape) and in the absence of catalyst (Control, blue shape). The absorption of MO was monitored at 464 nm . Note: Small bars are overlapped by the symbols ($n = 3$).

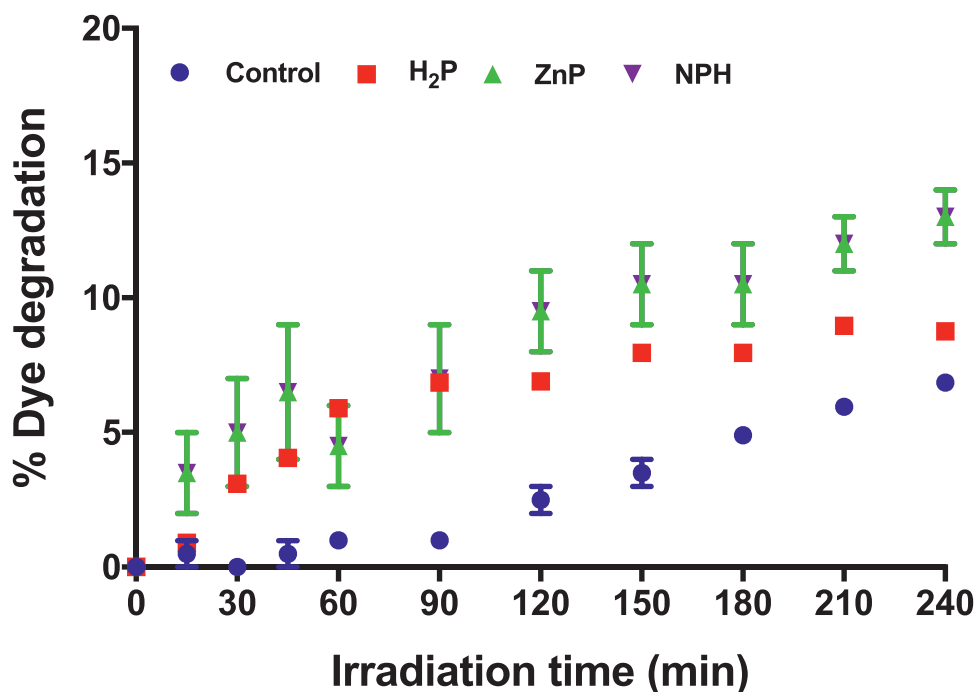


Fig. 6. Degradation of methyl orange (MO) under dark conditions at different reaction times: in the presence of aqueous H_2O_2 (0.25 mol L^{-1}) and $0.5 \text{ }\mu\text{M}$ of H_2P (red bars); $0.5 \text{ }\mu\text{M}$ of ZnP (green bars); $5.0 \text{ }\mu\text{M}$ of ZnP in NPH (purple bars) and with no catalyst (Control, blue bars). The MO absorbance was monitored at 464 nm . Note: Small bars are overlapped by the symbols ($n = 3$).

and after being irradiated, respectively. The results in show that in the absence of light (dark conditions) and after 90 min of reaction in the presence of any of the catalysts and H_2O_2 only 7% of MO was oxidized. After 270 min of reaction this value reached 13% for ZnP and NPH while for H_2P the value remains almost constant (ca 8%) and was similar to that observed for the control assay (reaction performed in the presence of H_2O_2 only). These results indi-

cate that there is no remarkable difference between the different catalysts when dye degradation is performed in the presence of H_2O_2 but in the absence of light.

The results in Fig. 6 show that the profile of these reactions in the presence of aqueous H_2O_2 is totally different when carried out under light irradiation. In fact, the action of light was particularly relevant for improving the rate of oxidation mediated by NPH

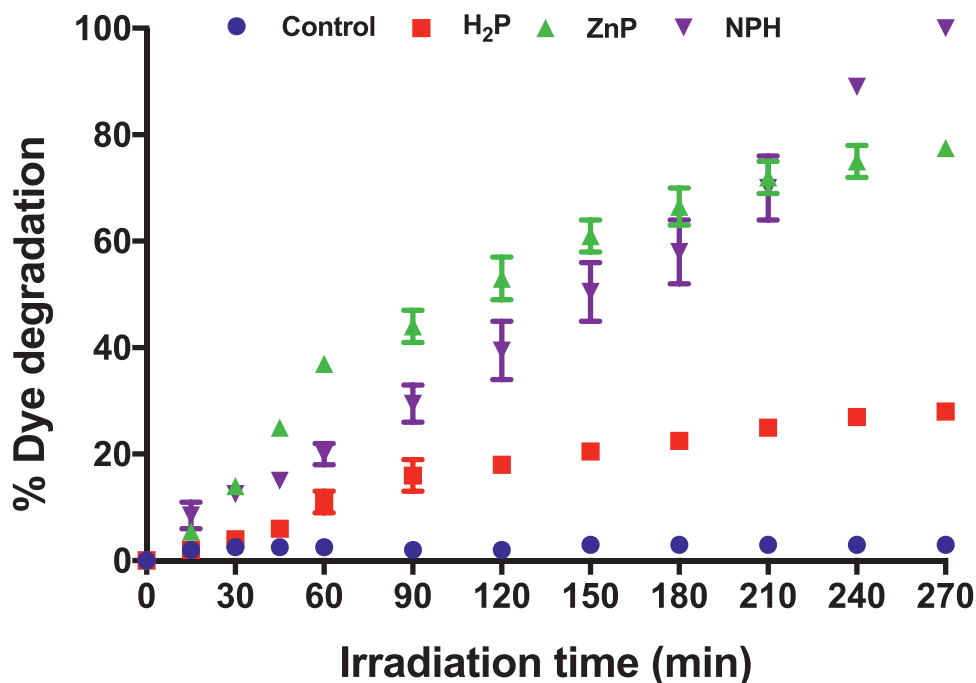


Fig. 7. Photocatalytic degradation of methyl orange (MO) in the presence of aqueous H₂O₂ (0.25 mol L⁻¹) at different irradiation times (irradiation with white light at an irradiance of 150 mW cm⁻²) in the presence of 0.5 μM of H₂P (red bars); 0.5 μM of ZnP (green bars); 5.0 μM of ZnP in NPH (purple bars) and in the absence of any catalyst (Control, blue shape). The MO absorbance was monitored at 464 nm. Note: Small bars are overlapped by the symbols. Note: Small bars are overlapped by the symbols (n = 3).

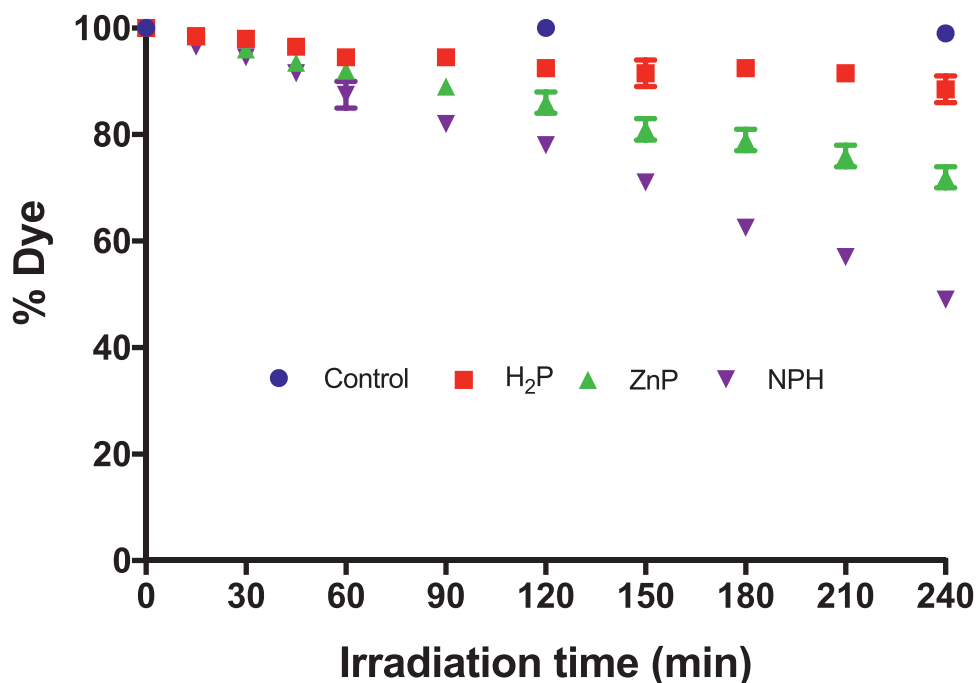


Fig. 8. Photocatalytic degradation of methyl orange (MO) in the presence of aqueous H₂O₂ (0.25 mol L⁻¹) and mannitol (0.1 mol L⁻¹) at different irradiation times (irradiation with white light at an irradiance of 150 mW cm⁻²) mediated by 0.5 μM of H₂P (red bars), 0.5 μM of ZnP (green bars) and 5.0 μM of ZnP in NPH (purple bars). The blue bars represent the control reaction (only hydrogen peroxide and mannitol). The band of MO was monitored at 464 nm. Note: Small bars are overlapped by the symbols (n = 3).

(100% after 270 min) and ZnP (75% after 270 min). When compared with the photoreactions performed under light irradiation but in absence of H₂O₂ (Fig. 5), an increment of ca 46% in catalytic activity was achieved for NPH, 56% for ZnP and 12.5% for H₂P. So, the beneficial effect of H₂O₂ in MO photodegradation is obvious when the results are compared with those obtained in its absence (Figs. 5 and Fig. 7).

The photodegradation of MO in the presence of ZnP, NPH and H₂O₂ showed to be time-dependent. This time dependence was also observed for NPH in the absence of H₂O₂. In fact, a longer contact time with the photocatalyst can facilitate the interaction of MO with the oxidation promoting species. The pathway responsible for MO photodegradation after photocatalyst activation by white light in the presence of molecular oxygen (O₂) can involve

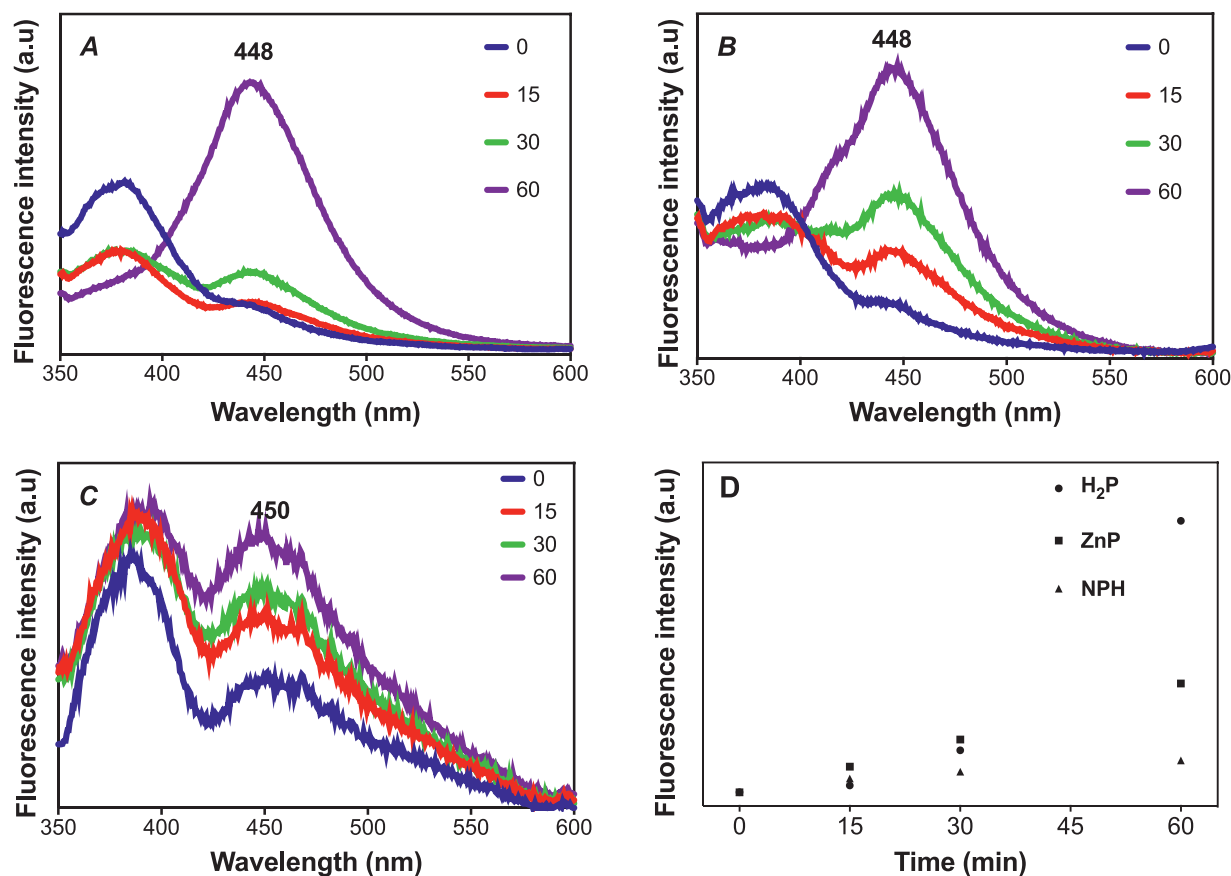


Fig. 9. Emission spectra ($\lambda_{\text{exc}} = 315 \text{ nm}$) obtained during the photolysis of TA (1.0 mM) at different irradiations times in the presence of H_2O_2 (0.25 mol L^{-1}) and (A) $0.5 \mu\text{M H}_2\text{P}$, (B) $0.5 \mu\text{M ZnP}$ and (C) $5.0 \mu\text{M}$ of ZnP in NPH ; all the irradiations were performed under white light at an irradiance of 150 mW cm^{-2} in PBS solutions ($\text{pH} = 7.0$) with 1% DMSO. (D) Evolution of HTA formation during the photolysis of TA for 60 min in the presence of $0.5 \mu\text{M H}_2\text{P}$, $0.5 \mu\text{M ZnP}$ and $5.0 \mu\text{M}$ of ZnP in NPH .

ROS such as hydrogen peroxide, superoxide and hydroxyl radicals (type I photochemical pathway) and/or singlet oxygen (photochemical pathway type II). Additionally, the decomposition of H_2O_2 through a Fenton-like reaction can be facilitated in the presence of NPH affording hydroxyl radicals [46]. The results show that the photocatalytic activity of H_2P , ZnP and NPH cannot be justified only by their efficiency to produce $^1\text{O}_2$ ($\text{H}_2\text{P} > \text{ZnP} > \text{NPH}$) and probably other highly reactive species such as hydroxyl radical ($\bullet\text{OH}$) are also involved. In order to verify if the production of $\bullet\text{OH}$ is also involved in the photocatalytic degradation of MO , the reactions in the presence of H_2O_2 were carried out in the presence of mannitol, an effective radical scavenger for $\bullet\text{OH}$ (Fig. 8) [47].

In fact, the photocatalytic efficacy of ZnP and NPH was strongly affected by the presence of mannitol confirming the role of $\bullet\text{OH}$ radicals in MO photodegradation (Fig. 8). These results obtained with hydrogen peroxide in the presence of mannitol are similar to the ones obtained when the reactions were performed without hydrogen peroxide (see Fig. 5).

Terephthalic acid (TA) has been used to indirectly measure the production of $\bullet\text{OH}$ by fluorescence. The $\bullet\text{OH}$ radical species react with TA to yield an intensely fluorescent mono-hydroxylated derivative (HTA). Fig. 9 shows the production of HTA in a phosphate buffer solution (PBS, $\text{pH} = 7.0$) with H_2O_2 in the presence of H_2P , ZnP and NPH under white light irradiation at different periods of irradiation. Upon irradiation, hydroxyl radicals are produced, yielding a high HTA fluorescence signal. All the photocatalysts are able to generate $\bullet\text{OH}$ radical in the presence H_2O_2 and under light, as indicated by the oxidation of the TA probe. Several studies [46] have shown that the TA probe have strong affinity for

iron oxide surfaces resulting in lower concentration of the highly fluorescent HTA (Fig. 9D). The fluorescence pattern observed during the irradiation of TA in the presence of NPH (Fig. 9C) is due to the interaction between the nanoparticles' surface and TA. It is worth to mention that in the absence of hydrogen peroxide, the HTA signal is not observed.

These results suggest that the photocatalytic mechanism involves mainly two ROS species, namely singlet oxygen and hydroxyl radical. At the end of the photocatalytic reaction using NPH , when total degradation of MO was observed, fresh solutions of MO and H_2O_2 were added to the reaction and subjected to the same reaction conditions of the first use. Again, total degradation of MO was observed after 240 min. Indeed, it was possible to reuse NPH at least three times without any loss of catalyst activity.

4. Conclusions

Core-shell magnetite-silica nanoparticles decorated with a porphyrin bearing meso-aryl groups with *N*-tosylethylenediamine residues can be considered an excellent photocatalyst to be used for dyes degradation. The NPH material turned out to be an effective photocatalyst, with higher photostability and the advantage of possible reuse. Additionally, the photocatalytic activity was improved with the addition of aqueous hydrogen peroxide. In this case, two mechanisms (type I and type II) can be involved in the MO photodegradation. The efficacy of this new photocatalytic material in the photodegradation of other dyes will be evaluated in future work.

Declaration of Competing Interest

The authors declare that they have no known competing financial interests or personal relationships that could have appeared to influence the work reported in this paper.

Acknowledgements

Thanks are due to CNPq (Conselho Nacional de Desenvolvimento Científico e Tecnológico) and CAPES (Coordenação de Aperfeiçoamento de Pessoal de Nível Superior). The authors also acknowledge the University of Aveiro and FCT/MCTES (Fundação para a Ciência e Tecnologia and Ministério da Ciência, Tecnologia e Ensino Superior) and European Union (COMPETE and FEDER programs) for the financial support of UIDB/50006/2020 (LAQV-REQUIMTE), UIDB/50011/2020 & UIDP/50011/2020 (CICECO) and UIDB/00100/2020 (CQE) research units and to the project COP2P (PTDC/QUI-QOR/30771/2017), through national funds and, when applicable, co-financed by FEDER—Operational Thematic Program for Competitiveness and Internationalization—COMPETE 2020, within the PT2020 Partnership Agreement. K. A. D. F. Castro thanks CNPq for her post-doctoral scholarship (Process 201107/2014-7) and J. M. M. Rodrigues acknowledges funding in the form of a Junior Researcher Contract under the scope of the project COP2P (PTDC/QUI-QOR/30771/2017).

Supplementary materials

Supplementary material associated with this article can be found, in the online version, at doi:10.1016/j.jorganchem.2021.121751.

References

- P. Zucca, C.M.B. Neves, M.M.Q. Simões, Maria da Graça P.M.S. Neves, G. Cocco, E. Sanjust, Immobilized Lignin Peroxidase-Like Metalloporphyrins as Reusable Catalysts in Oxidative Bleaching of Industrial Dyes, *Molecules* 21 (7) (2016) 964.
- M. Bartolomeu, M. Neves, M.A.F. Faustino, A. Almeida, Wastewater chemical contaminants: remediation by advanced oxidation processes, *Photochem. Photobiol. Sci.* 17 (11) (2018) 1573–1598.
- M.A. Al-Ghouti, M.A.M. Khraisheh, S.J. Allen, M.N. Ahmad, The removal of dyes from textile wastewater: a study of the physical characteristics and adsorption mechanisms of diatomaceous earth, *J. Environ. Manag.* 69 (3) (2003) 229–238.
- R. Bonnett, M.A. Krysteva, I.G. Lalov, S.V. Artarsky, Water disinfection using photosensitizers immobilized on chitosan, *Water Res* 40 (6) (2006) 1269–1275.
- T.K. Saha, H. Frauendorf, M. John, S. Dechert, F. Meyer, Efficient Oxidative Degradation of Azo Dyes by a Water-Soluble Manganese Porphyrin Catalyst, *ChemCatChem* 5 (3) (2013) 796–805.
- W. Przystas, E. Zablocka-Godlowska, E. Grabinska-Sota, Efficiency of decolorization of different dyes using fungal biomass immobilized on different solid supports, *Braz. J. Microbiol.* 49 (2) (2018) 285–295.
- S. Farias, D. Oliveira, A.A.U. Souza, S.M.A. Guelli U. de Souza, A.F. Morgado, Removal of reactive blue 21 and reactive red 195 dyes using horseradish peroxidase as catalyst, *Braz. J. Chem. Eng.* 34 (2017) 701–707.
- C. Galindo, P. Jacques, A. Kalt, Photodegradation of the aminoazobenzene acid orange 52 by three advanced oxidation processes: UV/H₂O₂, UV/TiO₂ and VIS/TiO₂: Comparative mechanistic and kinetic investigations, *J. Photochem. Photobiol. A* 130 (1) (2000) 35–47.
- R. Raliya, C. Avery, S. Chakrabarti, P. Biswas, Photocatalytic degradation of methyl orange dye by pristine titanium dioxide, zinc oxide, and graphene oxide nanostructures and their composites under visible light irradiation, *Appl. Nanosci.* 7 (5) (2017) 253–259.
- V.P. Barros, M.D. Assis, Iron porphyrins as biomimetic models for disperse azo dye oxidation, *J. Braz. Chem. Soc.* 24 (2013) 830–836.
- K.A.D.F. Castro, S. Silva, P.M. Pereira, M.M.Q. Simões, Maria da Graça P.M.S. Neves, J.A.S. Cavaleiro, F. Wypych, J.P. Tomé, S. Nakagaki, Galactodendritic porphyrinic conjugates as new biomimetic catalysts for oxidation reactions, *Inorg. Chem* 54 (9) (2015) 4382–4393.
- S. Nakagaki, K.A.D.F. Castro, Maria da Graça P.M.S. Neves, M.A. Faustino, Y. Iamamoto, The Research on Porphyrins and Analogues in Brazil: A Small Review Covering Catalytic and other Applications since the Beginning at Universidade de São Paulo in Ribeirão Preto until the Joint Venture between Brazilian Researchers and Colleagues from Universidade de Aveiro, Portugal, *J. Braz. Chem. Soc.* 30 (12) (2019) 2501–2535.
- M.M.Q. Simões, I.C.M.S. Santos, Maria da Graça P.M.S. Neves, A.M.V. Cavaleiro, J.A.S. Cavaleiro, J.L. Pombeiro (Ed.), Functionalization of sp² and sp³ Carbon Centers Catalyzed by Polyoxometalates and Metalloporphyrins, *Advances in Organometallic Chemistry and Catalysis* (2013) 59–71.
- K.C.M. Westrup, R.M. da Silva, K.M. Mantovani, L. Bach, J.F. Stival, P.G.P. Zamora, F. Wypych, G.S. Machado, S. Nakagaki, Light-assisted cyclohexane oxidation catalysis by a manganese(III) porphyrin immobilized onto zinc hydroxide salt and zinc oxide obtained by zinc hydroxide salt hydrothermal decomposition, *Appl. Catal. A* 602 (2020) 117708.
- M.M.Q. Simões, S.M.G. Pires, Maria da Graça P.M.S. Neves, J.A.S. Cavaleiro, Oxidative Transformations of Organic Compounds Mediated by Metalloporphyrins as Catalysts, *Handbook of Porphyrin Science*, pp. 197–306.
- S.L.H. Rebelo, A.M.N. Silva, C.J. Medforth, C. Freire, Iron(III) Fluorinated Porphyrins: Greener Chemistry from Synthesis to Oxidative Catalysis Reactions, *Molecules* 21 (4) (2016) 481.
- F.S. Vinhado, M.E.F. Gandini, Y. Iamamoto, A.M.G. Silva, M.M.Q. Simões, Maria da Graça P.M.S. Neves, A.C. Tomé, S.L.H. Rebelo, A.M.V.M. Pereira, J.A.S. Cavaleiro, Novel Mn(III)chlorins as versatile catalysts for oxyfunctionalisation of hydrocarbons under homogeneous conditions, *J. Mol. Catal. A Chem.* 239 (1–2) (2005) 138–143.
- S.L.H. Rebelo, S.M.G. Pires, M.M.Q. Simões, C.J. Medforth, J.A.S. Cavaleiro, Maria da Graça P.M.S. Neves, A Green and Versatile Route to Highly Functionalized Benzofurans Derivatives Using Biomimetic Oxygenation, *ChemistrySelect* 3 (5) (2018) 1392–1403.
- S.M.G. Pires, M.M.Q. Simões, I.C.M.S. Santos, S.L.H. Rebelo, M.M. Pereira, Maria da Graça P.M.S. Neves, J.A.S. Cavaleiro, Biomimetic oxidation of organosulfur compounds with hydrogen peroxide catalyzed by manganese porphyrins, *Appl. Catal. A* 439–440 (2012) 51–56.
- S.L.H. Rebelo, M.M.Q. Simões, Maria da Graça P.M.S. Neves, A.M.S. Silva, J.A.S. Cavaleiro, An efficient approach for aromatic epoxidation using hydrogen peroxide and Mn(III) porphyrins, *Chem. Commun.* (5) (2004) 608–609.
- K.A.D.F. Castro, G.T.P. Brancini, L.D. Costa, J. Biazzoto, M.A. Faustino, A. Tomé, Maria da Graça P.M.S. Neves, A. Almeida, M.R. Hamblin, R.S. da Silva, G. Braga, Efficient photodynamic inactivation of *Candida albicans* by a porphyrin and potassium iodide co-encapsulated in micelles, *Photochem. Photobiol. Sci.* 19 (2020) 1063–1071.
- L.D. Costa, J.A. Silva, S.M. Fonseca, C.T. Arranja, A.M. Urbano, A.J. Sobral, Photochemical Characterization and in Vitro Phototoxicity Evaluation of 5,10,15,20-Tetra(quinolin-2-yl)porphyrin as a Potential Sensitizer for Photodynamic Therapy, *Molecules* 21 (4) (2016) 439.
- K.A.D.F. Castro, N.M.M. Moura, M.M.Q. Simões, J.A.S. Cavaleiro, M.A.F. Faustino, A. Cunha, F.A. Almeida Paz, R.F. Mendes, A. Almeida, C.S.R. Freire, C. Vilela, A.J.D. Silvestre, S. Nakagaki, Maria da Graça P.M.S. Neves, Synthesis and characterization of photoactive porphyrin and poly(2-hydroxyethyl methacrylate) based materials with bactericidal properties, *Appl. Mater. Today* 16 (2019) 332–341.
- R.W. Redmond, J.N. Gamlin, A compilation of singlet oxygen yields from biologically relevant molecules, *Photochem. Photobiol.* 70 (4) (1999) 391–475.
- J.C. Barona-Castaño, C.C. Carmona-Vargas, T.J. Brocksom, K.T. de Oliveira, Porphyrins as Catalysts in Scalable Organic Reactions, *Molecules* 21 (3) (2016) 310.
- C.M.B. Neves, O.M.S. Filipe, N. Mota, S.A.O. Santos, A.J.D. Silvestre, E.B.H. Santos, Maria da Graça P.M.S. Neves, M.M.Q. Simões, Photodegradation of metoprolol using a porphyrin as photosensitizer under homogeneous and heterogeneous conditions, *J. Hazard Mater.* 370 (2019) 13–23.
- L. Fernandez, V.I. Esteves, A. Cunha, R.J. Schneider, J.P.C. Tomé, Photodegradation of organic pollutants in water by immobilized porphyrins and phthalocyanines, *J. Porphyrins Phthalocyanines* 20 (1–4) (2016) 150–166.
- O.M.S. Filipe, E.B.H. Santos, M. Otero, E.A.C. Gonçalves, Maria da Graça P.M.S. Neves, Photodegradation of metoprolol in the presence of aquatic fulvic acids. Kinetic studies, degradation pathways and role of singlet oxygen, OH radicals and fulvic acids triplet states, *J. Hazard. Mater.* 385 (2020) 121523.
- H. He, Y. Zhong, X. Liang, W. Tan, J. Zhu, C.Y. Wang, Natural Magnetite: an efficient catalyst for the degradation of organic contaminant, *Sci. Rep.* 5 (2015) 10139.
- M. Godoi, D.G. Liz, E.W. Ricardo, M.S.T. Rocha, J.B. Azeredo, A.L. Braga, Magnetite (Fe₃O₄) nanoparticles: an efficient and recoverable catalyst for the synthesis of alkynyl chalcogenides (selenides and tellurides) from terminal acetylenes and diorganyl dichalcogenides, *Tetrahedron* 70 (20) (2014) 3349–3354.
- H. Alina Maria, G. Alexandru Mihai, G. Monica Cartelle, M. Laurentiu, M. George Dan, Novel Drug Delivery Magnetite Nano-systems Used in Antimicrobial Therapy, *Curr. Org. Chem.* 18 (2) (2014) 185–191.
- G. Unsoy, U. Gunduz, O. Oprea, D. Ficai, M. Sonmez, M. Radulescu, M. Alexie, A. Ficai, Magnetite: from synthesis to applications, *Curr. Top. Med. Chem.* 15 (16) (2015) 1622–1640.
- I.L. Ardelean, L.B.N. Stoenca, D. Ficai, A. Ficai, R. Trusca, B.S. Vasile, G. Nechifor, E. Andronescu, Development of Stabilized Magnetite Nanoparticles for Medical Applications, *J. Nanomater.* 2017 (2017) 6514659.
- J. Chang, Q. Zhang, Y. Liu, Y. Shi, Z. Qin, Preparation of Fe₃O₄/TiO₂ magnetic photocatalyst for photocatalytic degradation of phenol, *J. Mater. Sci. Mater. Electron.* 29 (10) (2018) 8258–8266.
- K.-H. Choi, K.-K. Wang, E.P. Shin, S.-L. Oh, J.-S. Jung, H.-K. Kim, Y.-R. Kim, Water-Soluble Magnetic Nanoparticles Functionalized with Photosensitizer for Photocatalytic Application, *J. Phys. Chem. C* 115 (8) (2011) 3212–3219.

- [36] M. Neamțu, C. Nădejde, V.D. Hodoroaba, R.J. Schneider, U. Panne, Singlet oxygen generation potential of porphyrin-sensitized magnetite nanoparticles: Synthesis, characterization and photocatalytic application, *Appl. Catal. B: Environ.* 232 (2018) 553–561.
- [37] A.M.R. Gonsalves, J.M.T.B. Varejão, M.M. Pereira, Some new aspects related to the synthesis of meso-substituted porphyrins, *J. Heterocycl. Chem.* 28 (3) (1991) 635–640.
- [38] J.M. Rodrigues, A.S. Farinha, P.V. Muteto, S.M. Woranovicz-Barreira, F.A. Almeida Paz, Maria da Graça P.M.S. Neves, J.A. Cavaleiro, A.C. Tomé, M.T. Gomes, J.L. Sessler, J.P.C. Tomé, New porphyrin derivatives for phosphate anion sensing in both organic and aqueous media, *Chem. Commun.* 50 (11) (2014) 1359–1361.
- [39] C.M.B. Carvalho, E. Alves, L. Costa, J.P.C. Tomé, M.A.F. Faustino, Maria da Graça P.M.S. Neves, A.C. Tomé, J.A.S. Cavaleiro, A. Almeida, A. Cunha, Z. Lin, J. Rocha, Functional cationic nanomagnet-porphyrin hybrids for the photoinactivation of microorganisms, *ACS Nano* 4 (12) (2010) 7133–7140.
- [40] L. Huang, G. Szewczyk, T. Sarna, M.R. Hamblin, Potassium Iodide Potentiates Broad-Spectrum Antimicrobial Photodynamic Inactivation Using Photofrin, *ACS Infect. Dis.* 3 (4) (2017) 320–328.
- [41] P. Battioni, E. Cardin, M. Louloudi, B. Schöllhorn, G.A. Spyroulias, D. Mansuy, T.G. Traylor, Metalloporphyrinosilicas: a new class of hybrid organic–inorganic materials acting as selective biomimetic oxidation catalysts, *Chem. Commun.* (17) (1996) 2037–2038.
- [42] K.A.D.F. Castro, F. Figueira, R.F. Mendes, F.A. Almeida Paz, Maria da Graça P.M.S. Neves, J.A.S. Cavaleiro, S. Nakagaki, J.P.C. Tomé, M.M.Q. Simões, Porphyrinic coordination polymer-type materials as heterogeneous catalysts in catechol oxidation, *Polyhedron* 158 (2019) 478–484.
- [43] J.L. Clark, J.E. Hill, I.D. Rettig, J.J. Beres, R. Ziniuk, T.Y. Ohulchanskyy, T.M. McCormick, M.R. Detty, Importance of Singlet Oxygen in Photocatalytic Reactions of 2-Aryl-1,2,3,4-tetrahydroisoquinolines Using Chalcogenorosamine Photocatalysts, *Organometallics* 38 (12) (2019) 2431–2442.
- [44] W. Spiller, H. Kliesch, D. Wöhrle, S. Hackbarth, B. Röder, G. Schnurpfeil, Singlet oxygen quantum yields of different photosensitizers in polar solvents and micellar solutions, *J. Porphyrins Phthalocyanines* 2 (2) (1998) 145–158.
- [45] M.Q. Mesquita, José C.J.M.D.S. Menezes, S.M.G. Pires, Maria da Graça P.M.S. Neves, M.M.Q. Simões, A.C. Tomé, J.A.S. Cavaleiro, A. Cunha, A.L. Daniela-da-Silva, A. Almeida, M.A.F. Faustino, Pyrrolidine-fused chlorin photosensitizer immobilized on solid supports for the photoinactivation of Gram negative bacteria, *Dyes Pigments* 110 (2014) 123–133.
- [46] G. Lyngsie, L. Krumina, A. Tunlid, P. Persson, Generation of hydroxyl radicals from reactions between a dimethoxyhydroquinone and iron oxide nanoparticles, *Sci. Rep.* 8 (1) (2018) 10834.
- [47] B. Shen, R.G. Jensen, H.J. Bohnert, Mannitol Protects against Oxidation by Hydroxyl Radicals, *Plant Physiol* 115 (2) (1997) 527–532.